Published OnlineFirst May 30, 2013; DOI: 10.1158/0008-5472.CAN-12-3814

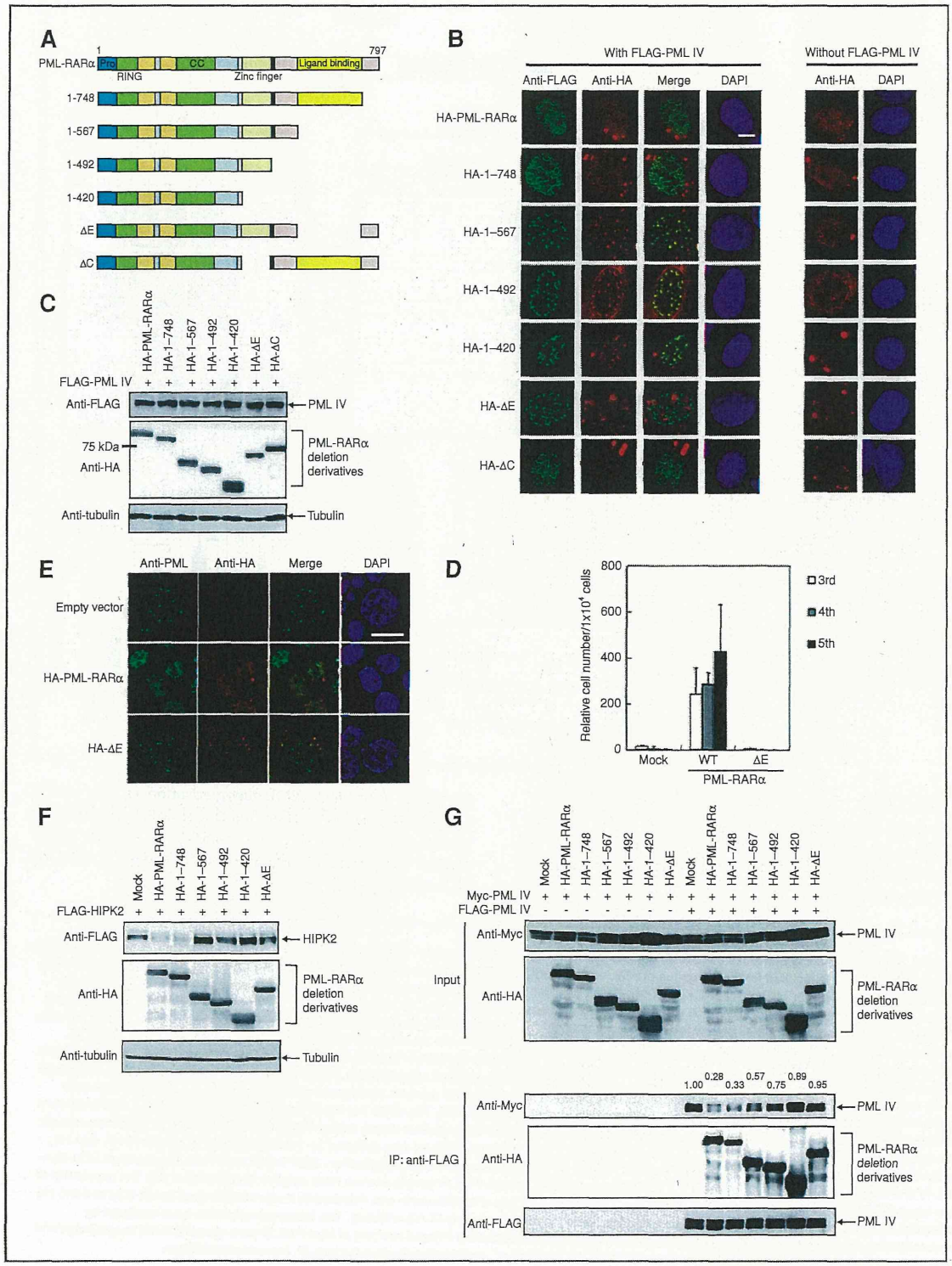

Published OnlineFirst May 30, 2013; DOI: 10.1158/0008-5472.CAN-12-3814

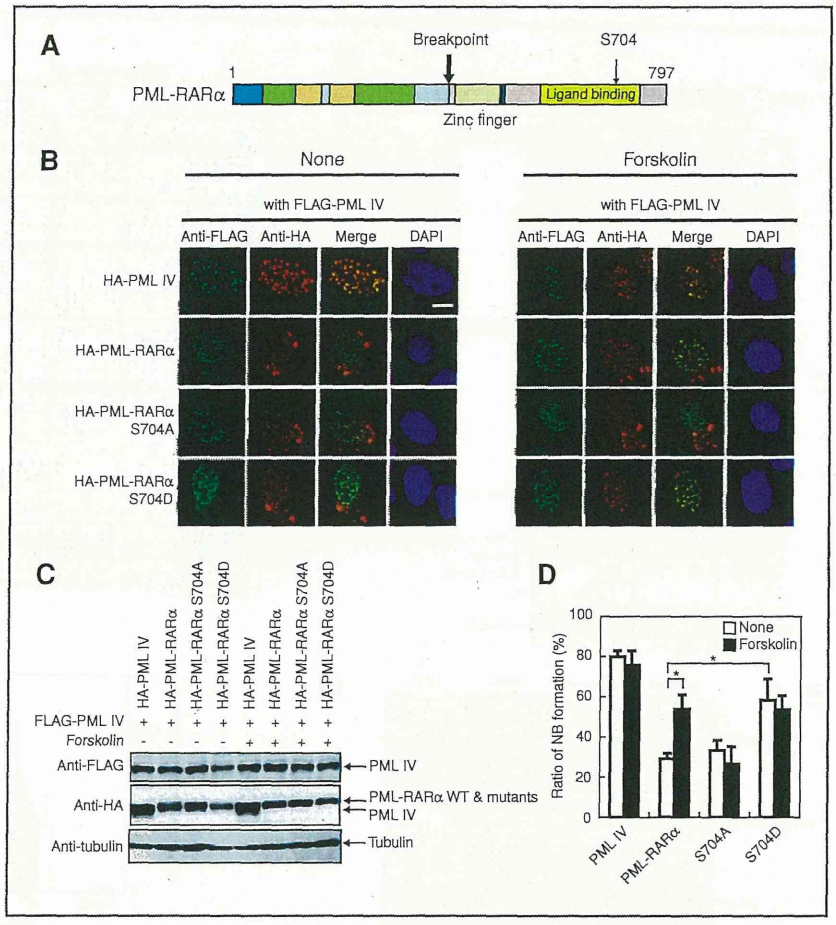

Figure 3. The PKA-dependent phosphorylation site of PML-RARα regulates PML nuclear body formation. A, diagram of the location of the PKA-dependent phosphorylation site of PML-RARα. B, phosphorylation of serine 704 is important for the restoration of PML nuclear bodies. FLAG-tagged PML IV and HA-tagged PML-RARα point mutants were coexpressed in U2OS cells. Cells were exposed to 50 μmol/L forskolin. PML nuclear bodies were analyzed using an anti-FLAG antibody. The white bar represents 10 μm. C, expression of PML-RARα wild-type and point mutants. The expression of PML IV (top), PML, PML-RARα wild-type or point mutants (middle), and tubulin (bottom) in U2OS cells was detected by immunoblot analysis with anti-FLAG, anti-HA, and anti-tubulin antibodies, respectively. D, quantification of nuclear body formation. The number of cells with PML nuclear bodies was counted. Values represent the mean ± SEM of 4 independent experiments. *, $P < 0.01$ compared with the PML-RARα value without forskolin. DAPI, 4′, 6-diamidino-2-phenylindole; NB, nuclear body.

Discussion

In more than 90% of APL cases, the PML-RARα fusion protein is generated by the t(15;17) chromosomal translocation. PML-RARα disrupts PML nuclear bodies by a mechanism that was not understood in detail. The present study reveals that PML-RARα blocks PML oligomerization, resulting in the disruption of nuclear bodies, and that cAMP/PKA phosphorylation of PML-RARα restores nuclear bodies. Our results suggest that nuclear body restoration enhances APL cell differentiation.

Figure 2. The ligand-binding domain of PML-RARα is essential for nuclear body disruption. A, diagram of PML-RARα deletion mutants. B, the ligand-binding domain of PML-RARα is required for the disruption of PML nuclear bodies. U2OS cells were transfected with pLNCX-FLAG-PML IV and pLNCX-HA-PML-RARα deletion constructs or only with pLNCX-HA-PML-RARα deletion constructs as described. PML nuclear bodies were analyzed using anti-FLAG antibody. The white bar represents 10 μm. C, expression of PML-RARα deletion mutants. The expression of PML IV (top), PML-RARα deletion mutants (middle), and tubulin (bottom) in U2OS cells was detected by immunoblotting using anti-FLAG, anti-HA, and anti-tubulin antibodies, respectively. D, the cells expressing PML-RARα ΔE are not immortalized. C-kit$^+$ mouse bone marrow cells were infected with empty vector (mock), pMSCV-HA-PML-RARα wild-type, or ΔE and cultured in methylcellulose medium. The colony number from the third to the fifth round of colonies is indicated (top). Values represent mean ± SEM from 3 independent experiments. E, PML-RARα ΔE does not inhibit nuclear body formation. C-kit$^+$ mouse bone marrow cells were infected with empty vector, pMSCV-HA-PML-RARα wild-type, or ΔE, and plated in methylcellulose medium. Endogenous murine PML nuclear bodies of the cells at first round of colonies were analyzed using mouse Pml-specific antibody (16.1–104). The white bar represents 10 μm. E, effect of PML-RARα deletion mutants on HIPK2 stability. 293FT cells were transfected with pLNCX-FLAG-HIPK2 and either empty vector or pLNCX-HA-PML-RARα deletion constructs. The expression of HIPK2 (top), PML-RARα deletion mutants (middle), and tubulin (bottom) was detected by immunoblotting using anti-FLAG, anti-HA, and anti-tubulin antibodies, respectively. G, effect of PML-RARα deletion mutants on PML oligomerization. 293FT cells were transfected with pLNCX-Myc-PML IV and either pLNCX-HA-PML-RARα deletion constructs or pLNCX-FLAG-PML IV (empty vectors were used as negative controls). The expression of Myc-tagged PML IV and HA-tagged PML-RARα deletion mutants in the lysates of transfectants was detected by immunoblotting using anti-Myc and anti-HA antibodies, respectively (input). The lysates of transfectants were incubated with anti-FLAG antibody. The immunoprecipitates were analyzed by immunoblotting using anti-Myc, anti-HA, and anti-FLAG antibodies (IP). The values of IP/input intensity of Myc-PML IV were quantified with ImageGauge and normalized to the value of Myc-PML IV/empty vector/FLAG-PML IV. DAPI, 4′, 6-diamidino-2-phenylindole; IP, immunoprecipitation.

Published OnlineFirst May 30, 2013; DOI: 10.1158/0008-5472.CAN-12-3814

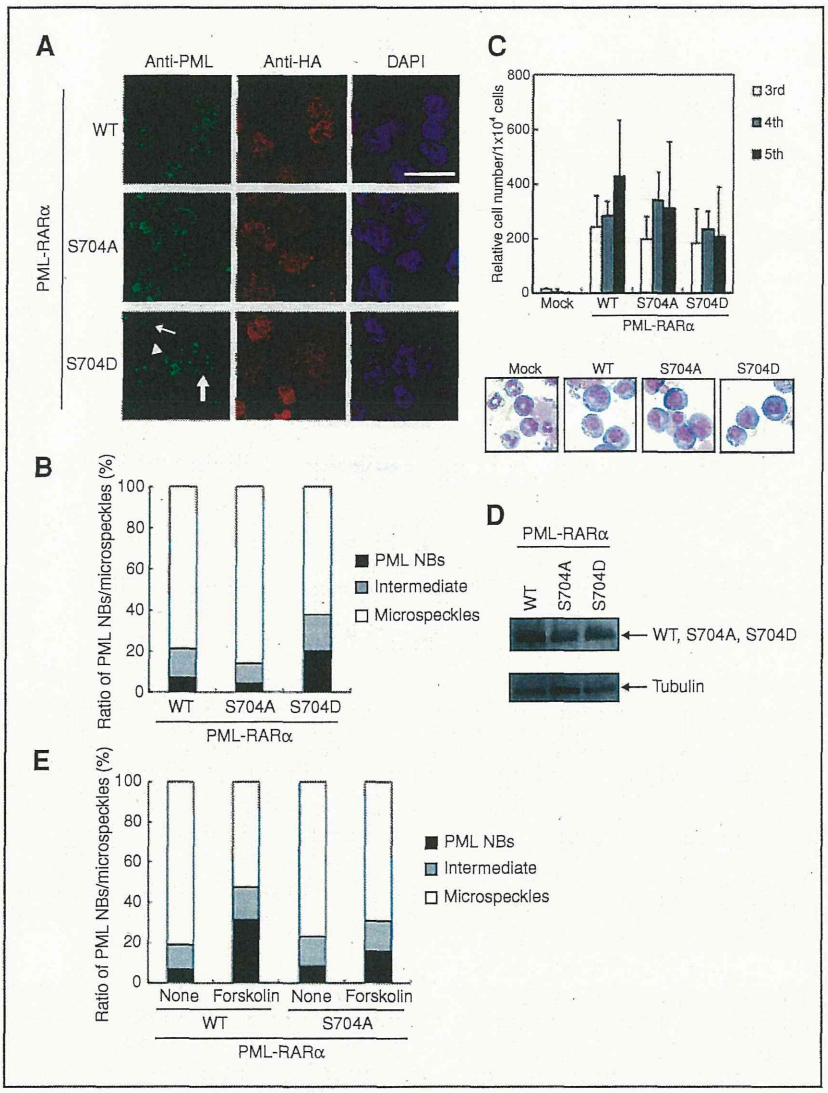

Figure 4. Nuclear body formation is maintained in cells stably expressing PML-RARα S704D. A, PML-RARα S704D does not inhibit nuclear body formation. C-kit$^+$ mouse bone marrow cells were infected with pMSCV-HA-PML-RARα wild-type, S704A, or S704D. Endogenous murine PML nuclear bodies of cells at the third round of colonies were analyzed using mouse Pml-specific antibody (16.1–104). The white bar represents 10 μm. The thick arrow represents PML nuclear bodies, arrowhead represents intermediate nuclear bodies, and thin arrow represents microspeckles. B, quantification of nuclear body formation. The number of cells with PML nuclear bodies, intermediate nuclear bodies, and microspeckles was counted. Values represent the average of 4 independent experiments. C, the cells expressing PML-RARα S704D are immortalized. C-kit$^+$ mouse bone marrow cells were infected with empty vector (mock), pMSCV-HA-PML-RARα wild-type, S704A, or S704D and cultured in methylcellulose medium. The colony number from the third to the fifth round of colonies is indicated (top). Values represent mean ± SEM from 3 independent experiments. The cells at the third round of colonies were stained with May–Giemsa stain (bottom). D, expression of PML-RARα wild-type, S704A, and S704D. The expression of wild-type PML-RARα and mutants and of tubulin in cells at the third round of colonies was analyzed by immunoblotting using anti-PML and anti-tubulin antibodies, respectively. E, quantification of nuclear body restoration. The cells expressing wild-type PML-RARα and S704A at the third round of colonies were collected and exposed to 50 μmol/L forskolin for 24 hours. Endogenous murine PML nuclear bodies were analyzed as described in A. The number of cells with PML nuclear bodies, intermediate nuclear bodies, or microspeckles was counted. Values represent the average of 4 independent experiments. DAPI, 4′, 6-diamidino-2-phenylindole; NB, nuclear body; WT, wild-type.

PML nuclear body disruption and restoration

Nuclear bodies are disrupted in APL cells harboring the t (15;17) chromosomal translocation (16, 17, 19). Results showed that wild-type PML-RARα blocked PML oligomerization (Supplementary Fig. S2C). Deletion analysis showed that PML-RARα mutants that block PML oligomerization

Published OnlineFirst May 30, 2013; DOI: 10.1158/0008-5472.CAN-12-3814

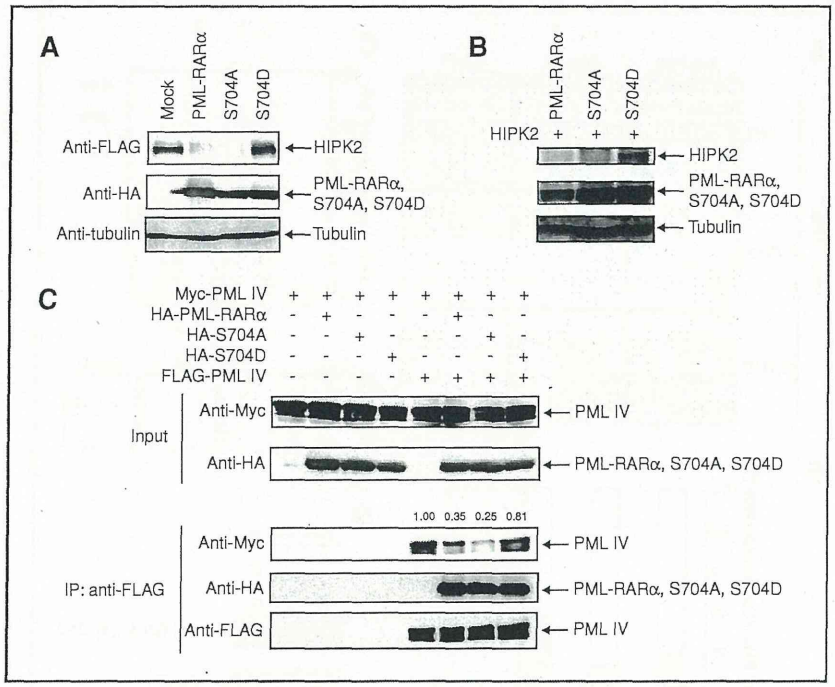

Figure 5. HIPK2 destabilization and inhibition of PML oligomerization are correlated with PML nuclear body disruption by PML-RARα. A, effect of the PML-RARα point mutants on HIPK2 stability. FLAG-tagged HIPK2 was expressed with either empty vector or HA-tagged PML-RARα point mutants. The expression of HIPK2 (top), PML-RARα point mutants (middle), and tubulin (bottom) was detected by immunoblotting using anti-FLAG, anti-HA, and anti-tubulin antibodies, respectively. B, effect of the PML-RARα point mutants on HIPK2 stability in a stable expression system. C-kit$^+$ mouse bone marrow cells were infected with pMSCV-HA-HIPK2 and pMSCV-HA-PML-RARα encoding either wild-type, S704A, or S704D. The expression of HIPK2, PML-RARα (wild-type and mutants), and tubulin at the third round of colonies was analyzed by immunoblotting using anti-HIPK2, anti-PML, and anti-tubulin antibodies, respectively. C, effect of the PML-RARα point mutants on PML oligomerization. 293FT cells were transfected with pLNCX-Myc-PML IV and either pLNCX-HA-PML-RARα substitution constructs or pLNCX-FLAG-PML IV (empty vectors were used as negative constructs). The expression of Myc-tagged PML IV and HA-tagged PML-RARα substitution mutants in the lysates of transfectants was detected by immunoblotting using anti-Myc and anti-HA antibodies, respectively (Input). The lysates of transfectants were incubated with anti-FLAG antibody. The immunoprecipitates were analyzed by immunoblotting using anti-Myc, anti-HA, and anti-FLAG antibodies (IP). The values of IP/Input intensity of Myc-PML IV were quantified with ImageGauge, and normalized to the value of Myc-PML IV/empty vector/FLAG-PML IV. IP, immunoprecipitation.

also disrupt nuclear bodies (Figs. 2B and G, 3B, and 5C). The blocking of PML oligomerization by PML-RARα occurs independent of their interaction (Figs 2G and 5C). These results suggest that the inability of inhibition of PML oligomerization by PML-RARα mutants is not due to the inability of interaction with PML IV, and imply that PML-RARα–induced nuclear body disruption is due to impaired PML oligomerization.

RARα and PML-RARα are phosphorylated by the cAMP/PKA pathway at a site located within the ligand-binding domain (29, 30). The PML-RARα S704D mutant, which is expected to simulate phosphorylated PML-RARα, did not block PML oligomerization and did not disrupt nuclear bodies. Moreover forskolin restored nuclear bodies disrupted in U2OS cells expressing wild-type PML-RARα (Fig. 3B and D), in mouse myeloid stem/progenitor cells expressing wild-type PML-RARα (Fig. 4E), or in APL-derived NB4 cells (Fig. 6D). Our results indicate that the ligand-binding domain of PML-RARα is key to the inhibition of PML oligomerization and to the disruption of PML nuclear bodies, and that PKA-dependent phosphorylation of the serine residue in that region reverses those effects and restores nuclear body formation. Phosphorylated PML-RARα is known to be easily degraded by ATRA (30); however, in the absence of ATRA, phosphorylated PML-RARα was stable (Figs. 4D, 5A and B, and Supplementary Fig. S6C). The mechanism by which phosphorylation of PML-RARα prevents its inhibition of PML oligomerization remains unclear. However, there are precedents for this; the phosphorylation of RARα by PKA enhances the interaction between RARα and cyclin H/cdk2 (29), suggesting that phosphorylation of RARα increases its interaction with cyclin H/cdk2. Thus, PML might find it easier to access a complex of phosphorylated PML-PML-RARα than a complex of dephosphorylated PML-PML-RARα.

Nuclear body restoration is important for differentiation of APL cells

The PKA phosphorylation site of PML-RARα regulates nuclear body formation. Forskolin restored nuclear bodies in

Published OnlineFirst May 30, 2013; DOI: 10.1158/0008-5472.CAN-12-3814

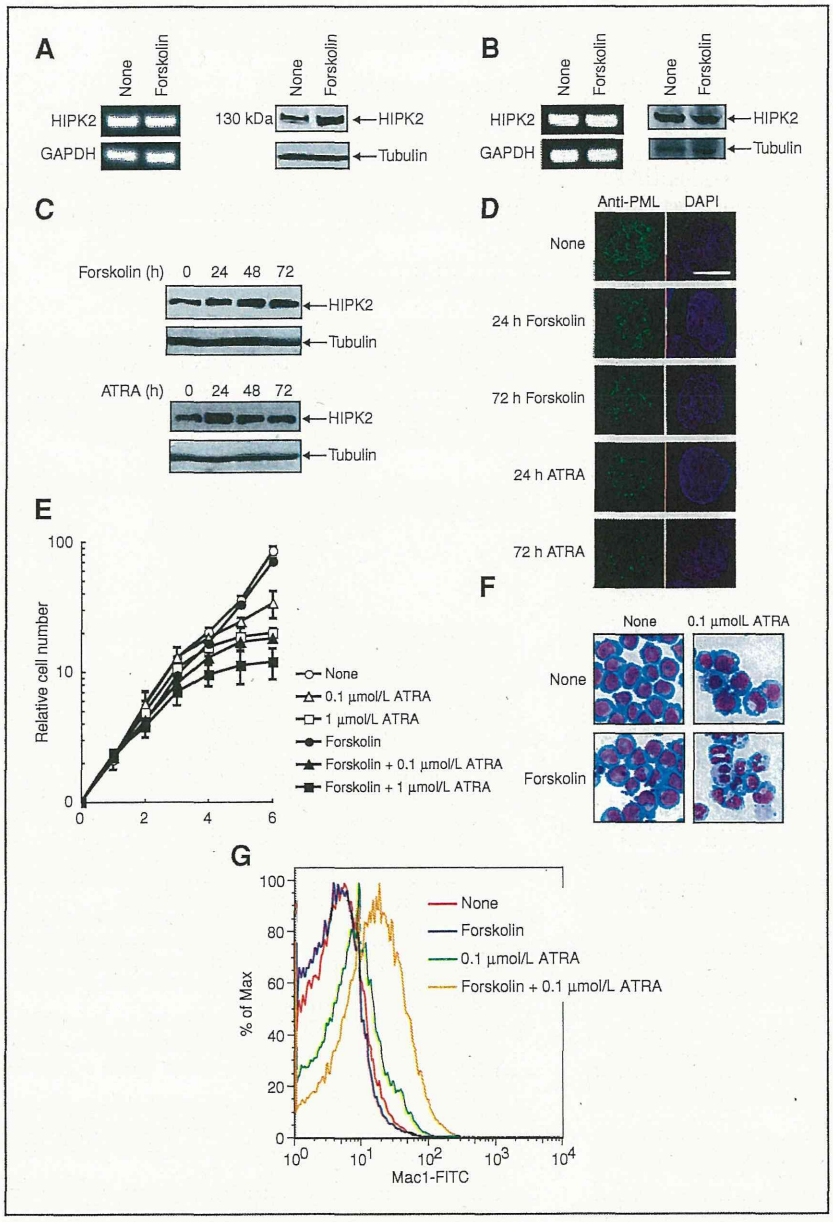

Figure 6. Nuclear body restoration promotes ATRA-induced APL cell differentiation. A, forskolin increases HIPK2 protein expression in NB4 cells. NB4 cells were treated with forskolin for 72 hours. The expression of HIPK2 and tubulin was analyzed by immunoblotting (right) using anti-HIPK2 and anti-tubulin antibodies, respectively. B, forskolin does not increase HIPK2 protein expression in K562 cells. The expression of HIPK2 and tubulin in K562 cells was analyzed as described in A. C, effect of forskolin or ATRA on HIPK2 expression. NB4 cells were treated with forskolin or ATRA for 24, 48, and 72 hours and were harvested. The lysates were analyzed as described in A. D, effect of forskolin or ATRA on nuclear body restoration. NB4 cells were exposed to forskolin or ATRA for 24 or 72 hours and stained with anti-PML antibody. The white bar represents 10 μm. E, growth curve of NB4 cells exposed to ATRA and/or forskolin. Cells were counted every other day for 6 days. Values were normalized to the value obtained at the zero time point. Values represent the mean ± SEM of 4 independent experiments. F, forskolin increases ATRA-induced NB4 cell differentiation. NB4 cells were stained with May–Giemsa stain 5 days after adding ATRA and/or forskolin. G, the combination of ATRA and forskolin increases the expression of Mac-1 in NB4 cells. NB4 cells were treated with ATRA and/or forskolin for 5 days, and incubated with anti-Mac-1-FITC. The cells were analyzed by flow cytometry.

APL-derived NB4 cells (Fig. 6D). Although forskolin alone was not sufficient to induce NB4 cell differentiation, it promoted ATRA-induced differentiation (Fig. 6G). Published studies showed that cAMP enhances retinoic acid-induced APL differentiation and PML-RARα transactivation (32–35). These studies also showed that PKA dissociates RARα from SMRT and activates transcription. Moreover, a recent report indicated that cAMP-dependent phosphorylation of PML-RARα was crucial for the eradication of APL-initiating cells (30). Taken together, these reports and the present data suggest that nuclear body restoration is one of the reasons why cAMP/PKA could be useful as an APL therapy.

We previously showed that HIPK2 is stabled in PML nuclear bodies and degraded outside of nuclear bodies by SCFFbx3, suggesting that HIPK2 is destabilized by disruption of nuclear bodies (15). In this paper, we showed that PML IV ΔCC, wild-type PML-RARα, PML-RARα 1–748, and S704A, which disrupted PML nuclear bodies, also destabilized HIPK2. In contrast, PML, PML-RARα 1–567, 1–492, 1–420, ΔE, and S704D, which did not disrupt nuclear bodies,

Published OnlineFirst May 30, 2013; DOI: 10.1158/0008-5472.CAN-12-3814

did not destabilize HIPK2. Forskolin and ATRA, which restore nuclear bodies in NB4 cells, increased HIPK2 expression (Fig. 6A and C), and the increase in HIPK2 expression was correlated with nuclear body restoration (Fig. 6D). These data indicate that HIPK2 destabilization is strongly correlated with nuclear body disruption and that nuclear body formation is important for HIPK2 stabilization. HIPK2 is important for PML-dependent transcriptional activation (15). We have also found that PML stabilizes the PU.1/p300 complex to regulate PU.1-dependent transcription and myeloid differentiation (26). Mutations of HIPK2 are found in AML and myelodysplastic syndrome (36). PML-RARα also disrupts PU.1/p300 complexes and inhibits myeloid differentiation (26). Therefore, nuclear body formation by PML oligomerization may lead to the recruitment of transcription factors/coactivators and to their stabilization for transcriptional activation and regulation of granulopoiesis. As suggested by the results of the present study, this might be because cAMP/PKA-dependent nuclear body restoration enhances APL cell differentiation.

Disclosure of Potential Conflicts of Interest

No potential conflicts of interest were disclosed.

Authors' Contributions

Conception and design: Y. Shima, I. Kitabayashi
Development of methodology: Y. Shima
Acquisition of data (provided animals, acquired and managed patients, provided facilities, etc.): Y. Shima, Y. Honma
Analysis and interpretation of data (e.g., statistical analysis, biostatistics, computational analysis): Y. Shima, I. Kitabayashi
Writing, review, and/or revision of the manuscript: Y. Shima, I. Kitabayashi

Acknowledgments

The authors thank Dr. de Thé for helpful discussions.

Grant Support

This work was supported in part by Grants-in-Aid from the Ministry of Health, Labor, and Welfare, the Ministry of Education, Culture, Sports, Science, and Technology, and National Cancer Center Research and Development Fund.

The costs of publication of this article were defrayed in part by the payment of page charges. This article must therefore be hereby marked *advertisement* in accordance with 18 U.S.C. Section 1734 solely to indicate this fact.

Received October 2, 2012; revised April 7, 2013; accepted April 22, 2013; published OnlineFirst May 30, 2013.

References

1. Gilliland DG. Molecular genetics of human leukemia. Leukemia 1998;12 Suppl 1:S7–12.
2. Look AT. Oncogenic transcription factors in the human acute leukemias. Science 1997;278:1059–64.
3. de Thé H, Chomienne C, Lanotte M, Degos L, Dejean A. The t(15;17) translocation of acute promyelocytic leukaemia fuses the retinoic acid receptor alpha gene to a novel transcribed locus. Nature 1990;347:558–61.
4. de Thé H, Lavau C, Marchio A, Chomienne C, Degos L, Dejean A. The PML-RAR alpha fusion mRNA generated by the t(15;17) translocation in acute promyelocytic leukemia encodes a functionally altered RAR. Cell 1991;66:675–84.
5. Goddard AD, Borrow J, Freemont PS, Solomon E. Characterization of a zinc finger gene disrupted by the t(15;17) in acute promyelocytic leukemia. Science 1991;254:1371–4.
6. Kakizuka A, Miller WH Jr, Umesono K, Warrell RP Jr, Frankel SR, Murty VV, et al. Chromosomal translocation t(15;17) in human acute promyelocytic leukemia fuses RAR alpha with a novel putative transcription factor, PML. Cell 1991;66:663–74.
7. Guo A, Salomoni P, Luo J, Shih A, Zhong S, Gu W, et al. The function of PML in p53-dependent apoptosis. Nat Cell Biol 2000;2:730–6.
8. Nguyen LA, Pandolfi PP, Aikawa Y, Tagata Y, Ohki M, Kitabayashi I. Physical and functional link of the leukemia-associated factors AML1 and PML. Blood 2005;105:292–300.
9. Pearson M, Carbone R, Sebastiani C, Cioce M, Fagioli M, Saito S, et al. PML regulates p53 acetylation and premature senescence induced by oncogenic Ras. Nature 2000;406:207–10.
10. Möller A, Sirma H, Hofmann TG, Rueffer S, Klimczak E, Droge W, et al. PML is required for homeodomain-interacting protein kinase 2 (HIPK2)-mediated p53 phosphorylation and cell cycle arrest but is dispensable for the formation of HIPK domains. Cancer Res 2003;63:4310–4.
11. von Mikecz A, Zhang S, Montminy M, Tan EM, Hemmerich P. CREB-binding protein (CBP)/p300 and RNA polymerase II colocalize in transcriptionally active domains in the nucleus. J Cell Biol 2000;150:265–73.
12. Weis K, Rambaud S, Lavau C, Jansen J, Carvalho T, Carmo-Fonseca M, et al. Retinoic acid regulates aberrant nuclear localization of PML-RAR alpha in acute promyelocytic leukemia cells. Cell 1994;76:345–56.
13. Ishov AM, Sotnikov AG, Negorev D, Vladimirova OV, Neff N, Kamitani T, et al. PML is critical for ND10 formation and recruits the PML-interacting protein daxx to this nuclear structure when modified by SUMO-1. J Cell Biol 1999;147:221–34.
14. Torii S, Egan DA, Evans RA, Reed JC. Human Daxx regulates Fas-induced apoptosis from nuclear PML oncogenic domains (PODs). EMBO J 1999;18:6037–49.
15. Shima Y, Shima T, Chiba T, Irimura T, Pandolfi PP, Kitabayashi I. PML activates transcription by protecting HIPK2 and p300 from SCFFbx3-mediated degradation. Mol Cell Biol 2008;28:7126–38.
16. Daniel MT, Koken M, Romagne O, Barbey S, Bazarbachi A, Stadler M, et al. PML protein expression in hematopoietic and acute promyelocytic leukemia cells. Blood 1993;82:1858–67.
17. Dyck JA, Maul GG, Miller WH Jr, Chen JD, Kakizuka A, Evans RM. A novel macromolecular structure is a target of the promyelocyte-retinoic acid receptor oncoprotein. Cell 1994;76:333–43.
18. Kastner P, Perez A, Lutz Y, Rochette-Egly C, Gaub MP, Durand B, et al. Structure, localization and transcriptional properties of two classes of retinoic acid receptor alpha fusion proteins in acute promyelocytic leukemia (APL): structural similarities with a new family of oncoproteins. EMBO J 1992;11:629–42.
19. Koken MH, Puvion-Dutilleul F, Guillemin MC, Viron A, Linares-Cruz G, Stuurman N, et al. The t(15;17) translocation alters a nuclear body in a retinoic acid-reversible fashion. EMBO J 1994;13:1073–83.
20. Chen GQ, Shi XG, Tang W, Xiong SM, Zhu J, Cai X, et al. Use of arsenic trioxide (As2O3) in the treatment of acute promyelocytic leukemia (APL): I. As2O3 exerts dose-dependent dual effects on APL cells. Blood 1997;89:3345–53.
21. Zhu J, Koken MH, Quignon F, Chelbi-Alix MK, Degos L, Wang ZY, et al. Arsenic-induced PML targeting onto nuclear bodies: implications for the treatment of acute promyelocytic leukemia. Proc Natl Acad Sci U S A 1997;94:3978–83.
22. Lin RJ, Evans RM. Acquisition of oncogenic potential by RAR chimeras in acute promyelocytic leukemia through formation of homodimers. Mol Cell 2000;5:821–30.
23. Minucci S, Maccarana M, Cioce M, De Luca P, Gelmetti V, Segalla S, et al. Oligomerization of RAR and AML1 transcription factors as a novel mechanism of oncogenic activation. Mol Cell 2000;5:811–20.
24. Perez A, Kastner P, Sethi S, Lutz Y, Reibel C, Chambon P. PMLRAR homodimers: distinct DNA binding properties and heteromeric interactions with RXR. EMBO J 1993;12:3171–82.

Published OnlineFirst May 30, 2013; DOI: 10.1158/0008-5472.CAN-12-3814

25. Tagata Y, Yoshida H, Nguyen LA, Kato H, Ichikawa H, Tashiro F, et al. Phosphorylation of PML is essential for activation of C/EBP epsilon and PU.1 to accelerate granulocytic differentiation. Leukemia 2008;22:273–80.
26. Yoshida H, Ichikawa H, Tagata Y, Katsumoto T, Ohnishi K, Akao Y, et al. PML-retinoic acid receptor alpha inhibits PML IV enhancement of PU.1-induced C/EBPepsilon expression in myeloid differentiation. Mol Cell Biol 2007;27:5819–34.
27. Jeanne M, Lallemand-Breitenbach V, Ferhi O, Koken M, Le Bras M, Duffort S, et al. PML/RARA oxidation and arsenic binding initiate the antileukemia response of As2O3. Cancer Cell 2010;18:88–98.
28. Grignani F, Testa U, Rogaia D, Ferrucci PF, Samoggia P, Pinto A, et al. Effects on differentiation by the promyelocytic leukemia PML/RARalpha protein depend on the fusion of the PML protein dimerization and RARalpha DNA binding domains. EMBO J 1996;15:4949–58.
29. Gaillard E, Bruck N, Brelivet Y, Bour G, Lalevee S, Bauer A, et al. Phosphorylation by PKA potentiates retinoic acid receptor alpha activity by means of increasing interaction with and phosphorylation by cyclin H/cdk7. Proc Natl Acad Sci U S A 2006;103:9548–53.
30. Nasr R, Guillemin MC, Ferhi O, Soilihi H, Peres L, Berthier C, et al. Eradication of acute promyelocytic leukemia-initiating cells through PML-RARA degradation. Nat Med 2008;14:1333–42.
31. Duprez E, Lillehaug JR, Naoe T, Lanotte M. cAMP signalling is decisive for recovery of nuclear bodies (PODs) during maturation of RA-resistant t(15;17) promyelocytic leukemia NB4 cells expressing PML-RAR alpha. Oncogene 1996;12:2451–9.
32. Altucci L, Rossin A, Hirsch O, Nebbioso A, Vitoux D, Wilhelm E, et al. Rexinoid-triggered differentiation and tumor-selective apoptosis of acute myeloid leukemia by protein kinase A-mediated desubordination of retinoid X receptor. Cancer Res 2005;65:8754–65.
33. Duprez E, Lillehaug JR, Gaub MP, Lanotte M. Differential changes of retinoid-X-receptor (RXR alpha) and its RAR alpha and PML-RAR alpha partners induced by retinoic acid and cAMP distinguish maturation sensitive and resistant t(15;17) promyelocytic leukemia NB4 cells. Oncogene 1996;12:2443–50.
34. Guillemin MC, Raffoux E, Vitoux D, Kogan S, Soilihi H, Lallemand-Breitenbach V, et al. *In vivo* activation of cAMP signaling induces growth arrest and differentiation in acute promyelocytic leukemia. J Exp Med 2002;196:1373–80.
35. Kamashev D, Vitoux D, De Thé H. PML-RARA-RXR oligomers mediate retinoid and rexinoid/cAMP cross-talk in acute promyelocytic leukemia cell differentiation. J Exp Med 2004;199:1163–74.
36. Li XL, Arai Y, Harada H, Shima Y, Yoshida H, Rokudai S, et al. Mutations of the HIPK2 gene in acute myeloid leukemia and myelodysplastic syndrome impair AML1- and p53-mediated transcription. Oncogene 2007;26:7231–9.

Cancer Science
The official journal of the Japanese Cancer Association

Roles of AML1/RUNX1 in T-cell malignancy induced by loss of p53

Kimiko Shimizu,[1] Kazutsune Yamagata,[1] Mineo Kurokawa,[2] Shuki Mizutani,[3] Yukiko Tsunematsu[4] and Issay Kitabayashi[1,5]

[1]Division of Hematological Malignancy, National Cancer Center Research Institute, Tokyo; [2]Department of Internal Medicine, University of Tokyo Hospital, Tokyo; [3]Department of Pediatrics, Tokyo Medical and Dental University, Tokyo; [4]Division of Hematology, National Center for Child Health and Development, Tokyo, Japan

(Received November 14, 2012/Revised May 1, 2013/Accepted May 1, 2013/Accepted manuscript online May 17, 2013/Article first published online June 20, 2013)

***AML1/RUNX1* is a frequent target of chromosome translocations and mutations in myeloid and B-cell leukemias, and upregulation of AML1 is also observed in some cases of T-cell leukemias and lymphomas. This study shows that the incidence of thymic lymphoma in p53-null mice is less frequent in the *Aml1*$^{+/-}$ than in the *Aml1*$^{+/+}$ background. AML1 is upregulated in p53-null mouse bone-marrow cells and embryonic fibroblasts. In the steady state, p53 binds to and inhibits the distal *AML1* promoter. When the cells are exposed to stresses, p53 is released from the distal *AML1* promoter, resulting in upregulation of *AML1*. Overexpression of AML1 stimulates T-lymphocyte proliferation. These results suggest that upregulation of AML1 induced by loss of p53 promotes lymphoid-cell proliferation, thereby inducing lymphoma development. (*Cancer Sci* 2013; 104: 1033–1038)**

AML1, also known as the RUNX1 transcription factor, is encoded by one of the most frequently mutated genes in acute leukemia. The *AML1* gene is disrupted by translocations in leukemia.[1,2] AML1 is also inactivated by point mutations within its DNA-binding domain in both acute myeloid leukemia (AML)[3] and myelodysplastic syndromes (MDS).[4] *AML1* haploinsufficiency underlies familial platelet disorder, an inherited leukemia predisposition syndrome.[5] On the other hand, amplification of the locus containing *AML1* and overexpression of AML1 are observed in some cases of leukemias and lymphomas,[6–10] suggesting that an increased dosage of normal *AML1* may contribute to leukemogenesis.

The p53 tumor suppressor functions in the most important checkpoint-control pathway that prevents human cancer.[11] Although hematopoiesis in p53-null mice proceeds apparently normally, many studies have implicated p53 in the proliferation, differentiation, apoptosis, and aging of hematopoietic cells.[12–16] Moreover, p53 deletions and mutations are detected at high frequencies in blast crisis chronic myelogenous leukemia and acute leukemia, as well as in almost 50% of adult T-cell leukemias.[17,18] In the present study, we aimed to elucidate the relationship between AML1 and p53 in T-cell malignancy. Because the most frequent tumor to develop in p53-null mice is T-cell lymphoma,[19] we studied the role of AML1 in cancer development using the p53-null mouse as an animal model system of T-cell acute lymphoblastic leukemia (T-ALL).

Materials and Methods

Mice. *Aml1*$^{+/-}$ mice (a gift from T. Okuda) were mated to *p53*$^{+/-}$ mice (a gift from H. Koseki) to generate *Aml1*$^{+/-}$ *p53*$^{+/-}$ male mice. The mice were then mated to *p53*$^{+/-}$ female mice to generate *Aml1*$^{+/+}$ *p53*$^{-/-}$ or *Aml1*$^{+/-}$ *p53*$^{-/-}$ mice. For *in vitro* T-cell proliferation experiments, *Aml1*$^{fl/fl}$ mice[20] were mated to tamoxifen-inducible *ERT2-Cre* knock-in mice (Artemis Pharmaceuticals GmbH, Cologne, Germany)[21] to generate *Aml1*$^{fl/fl}$ *ERT2-Cre* mice. Active Cre-recombinase was induced by the addition of 50 nM 4-hydroxytamoxifen into the culture medium. The background of the mice used in this study is C57BL/6. The mice were kept at the Division of Animal Laboratory (National Cancer Center, Tokyo, Japan), according to institutional guidelines.

Quantitative RT-PCR. Total RNA extraction, reverse transcription, and quantitative PCR were performed using ISOGEN (Wako Chemical, Osaka, Japan); the High Capacity cDNA reverse transcription kit (Applied Biosystems, Foster City, CA, USA); and TaqMan probes for *RUNX1* (Hs00231079_m1), *RUNX3* (Hs00231709_m1), *TP53* (Hs01034249_m1), *Runx1* (Mm00486762_m1), *Runx2* (Mm0003003491_m1), *Runx3* (Mm00490666_m1), *Trp53* (Mm01731290_g1), *Pre T-cell antigen receptor alpha* (Mm00478363_m1), *Fas* (Mm00433237), and *18S* rRNA (Hs99999901_s1), purchased from (Applied Biosystems). Expression levels were normalized to those of *18S* rRNA.

Chromatin immunoprecipitation. ChIP analysis was performed as described,[22] using primary antibodies specific for p53 (sc-6243 and DO1) purchased from Santa Cruz Biotechnology (Santa Cruz, CA, USA) or antibodies for Histone H3 (ab1791), Histone H3 K4Me3 (ab8580), or Histone H3 K9Ac (ab4441) purchased from Abcam (Cambridge, MA, USA). Quantitative real-time PCR was performed on precipitated DNA using primers designed by PRIMER EXPRESS software (Applied Biosystems). The values relative to input were determined using a standard curve, and the relative quantification method was as described in ABI User Bulletin #2. The ChIP primer sequences corresponding to the mouse *Aml1* or human *AML1* distal promoter regions are available upon request.

T-cell proliferation assay. Number of living cells was determined by measuring ATP production using the Cell Titer Glo assay kit (Promega, Fitchburg, WI, USA) and a GLOMAX microplate luminometer (Promega).

Results

Dosage of *Aml1/Runx1* is critical for development of T-cell lymphoma in p53-null mice. Loss of the p53 allele and amplification or overexpression of the *AML1* gene is frequently observed in human lymphoblastic leukemia or lymphoma. Consistent with this, thymic lymphoma is the most frequent malignant disease in p53-null mice.[19] To analyze the effect of *Aml1* gene dosage on the generation of lymphoma, we generated *Aml1*$^{+/-}$ mice in a *p53*$^{-/-}$ background. We were unable to produce *Aml1*$^{-/-}$ *p53*$^{-/-}$ mice because the *Aml1*$^{-/-}$ mice died at embryonic days E11.5–E12.5, as reported.[23] We then compared the frequency of spontaneously occurring

[5]To whom correspondence should be addressed.
E-mail: ikitabay@ ncc.go.jp

doi: 10.1111/cas.12199

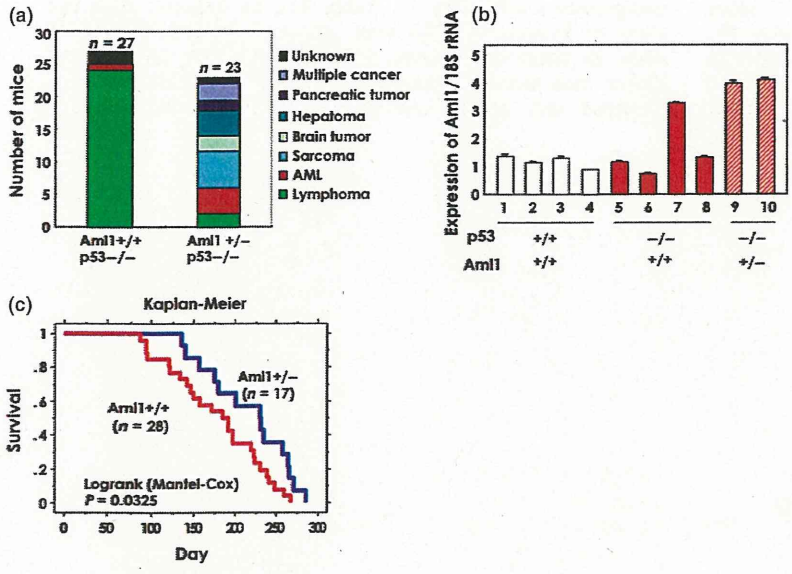

Fig. 1. *Aml1* haploinsufficiency in p53-null mice prevents the development of T-cell lymphoma. (a) Spontaneous onset of malignant transformation in p53-null mice of $Aml1^{+/+}$ and $Aml1^{+/-}$ genotypes. The majority of lymphomas developed in $Aml1^{+/+}$ mice were T-cell lymphomas (for details, see Table S1). (b) The level of *Aml1* transcripts in T-cell lymphoma. Total RNA of thymus from six mice with lymphoma (red bar, filled: $Aml1^{+/+}$ $p53^{-/-}$, red bar, diagonal stripes: $Aml1^{+/-}$ $p53^{-/-}$) and four normal controls (white) was isolated and quantitative reverse transcription-polymerase chain reaction (qRT-PCR) was performed as described in Experimental Procedures. The data shown are the means ± standard error of the mean (SEM). (c) Event-free survival curves for $p53^{-/-}$ $Aml1^{+/+}$ mice ($n = 28$) and $p53^{-/-}$ $Aml1^{+/-}$ mice ($n = 17$). Mice carrying sarcomas ($n = 6$) were not included in this analysis, because these mice were killed at the onset of disease. Statistical analysis was performed using the StatView software.

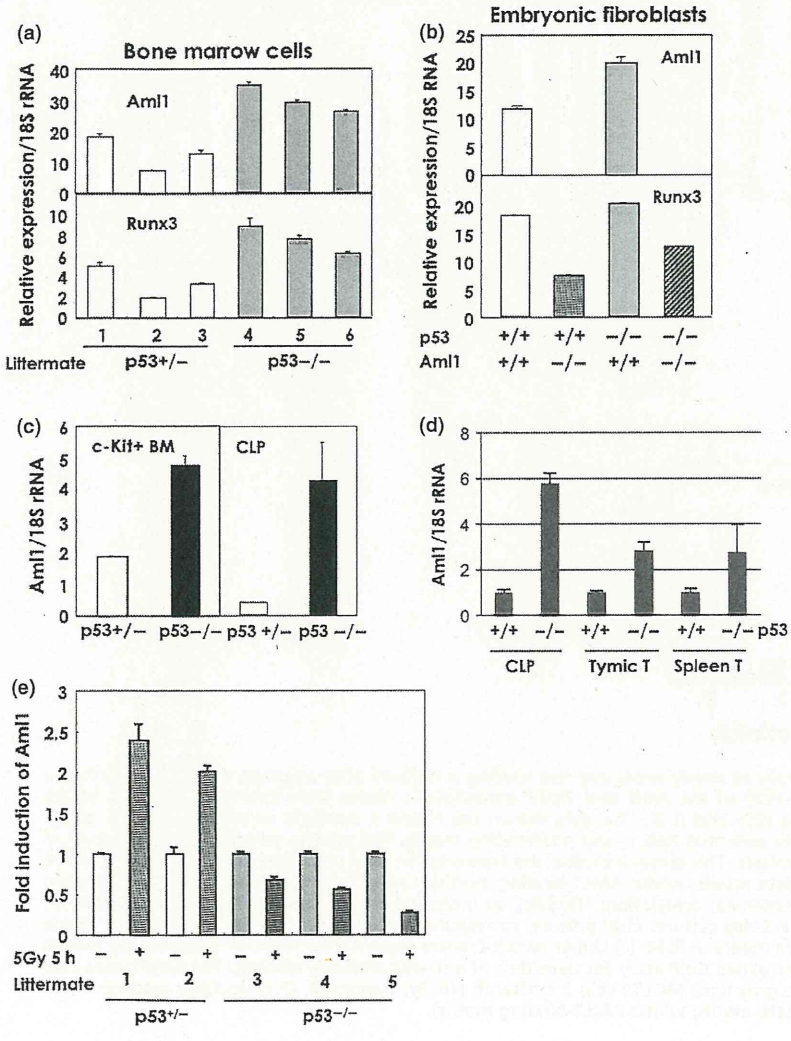

Fig. 2. AML1 is overexpressed in cells with p53-null mutations and is induced by stress. (a) *Aml1* is overexpressed in bone-marrow cells from p53-null mice in the steady state. The level of *Aml1* transcripts in bone marrow cells from littermate mice, generated by mating a $p53^{+/-}$ female and a $p53^{-/-}$ male mouse, was measured. Total RNA was prepared and subjected to quantitative reverse transcription-polymerase chain reaction (qRT-PCR) analysis of *Aml1*and *Runx3*. 1–3: $p53^{+/-}$ littermates, 4–6: $p53^{-/-}$ littermates. (b) *Aml1* is overexpressed in mouse embryonic fibroblast (MEF) cells from p53-null mice The level of *Aml1* and *Runx3* transcripts in the MEFs of the indicated phenotype was measured by qRT-PCR using total RNA of cells at the time of passage 2 as described in Experimental Procedures. MEF cells were isolated from littermate E11.5 embryos that were generated by crossing $Aml1^{+/-}$ male and $Aml1^{+/-}$ female mice of p53 wild type background. The data shown are the means ± standard error of the mean (SEM). (c) *Aml1* is overexpressed in bone marrow cells from p53-null mice. The level of *Aml1* transcripts,. and control *18S* rRNA, in c-Kit^{+} bone marrow cells and in the bone marrow CLP (c-Kit^{low}, $Sca1^{+}$, IL-$7Ra^{+}$, Lin^{-}) fraction of littermate mice, generated by mating a $p53^{+/-}$ female and a $p53^{-/-}$ male mouse. Total RNA was prepared and subjected to qRT-PCR for assay of *Aml1* and *18S* rRNA. The data shown are the means ± SEM. (d) *Aml1* is overexpressed in p53-null cells. Total RNA was isolated from c-Kit^{+} bone marrow (BM) cells, CLP, thymocytes, CD4+ splenic T cells, and MEFs, all of which were prepared from wild-type and $p53^{-/-}$ littermates. The level of *Aml1* transcripts was analyzed. The data shown are means ± SEM. (e) *Aml1* expression is also induced by IR in mouse cells. The level of *Aml1* transcripts was measured in bone-marrow cells from littermate mice, generated by mating a $p53^{+/-}$ female and a $p53^{-/-}$ male mouse. The cells were exposed to 5 Gy of IR and cultured for 5 h. Total RNA was prepared and subjected to semi-quantitative RT-PCR for analysis of *Aml1*. 1, 2: $p53^{+/-}$ littermates, 3–5: $p53^{-/-}$ littermates.

doi: 10.1111/cas.12199

tumors in *Aml1*$^{+/+}$ *p53*$^{-/-}$ mice and *Aml1*$^{+/-}$ *p53*$^{-/-}$ mice. Within a period of 40 weeks after birth, the majority of malignant disease (89%) in *Aml1*$^{+/+}$ *p53*$^{-/-}$ mice was T-cell lymphoma. However, in *Aml1*$^{+/-}$ *p53*$^{-/-}$ mice, a wide range of malignancies was observed, with sarcoma being the major malignancy (26%) (Fig. 1a, Table S1); by contrast, only two cases of lymphoma (9%) were observed in *Aml1*$^{+/-}$ *p53*$^{-/-}$ mice. In those lymphomas, the levels of *Aml1* mRNA were higher than those in normal T cells (Fig. 1b). Fluorescence-activated cell sorting and RT-PCR analyses revealed that

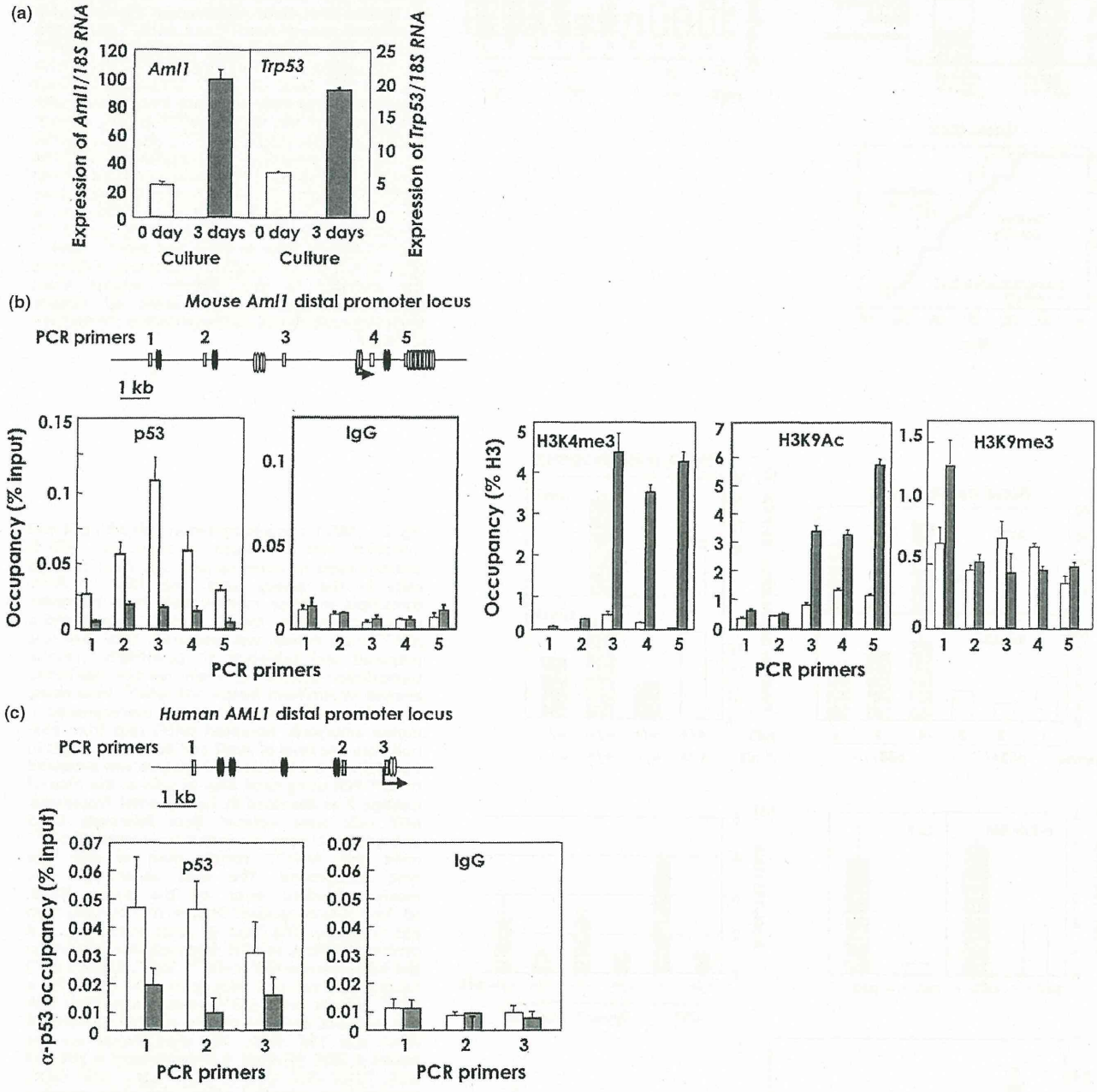

Fig. 3. p53 binds to the *AML1* promoter of hematopoietic cells at steady state, and the binding is reduced after exposure to stresses. (a) Quantitative reverse transcription-polymerase chain reaction (qRT-PCR) of the *Aml1* and *Trp53* transcripts in mouse bone-marrow c-Kit$^+$ cells before (0 day) or after (3 day) 3-day *in vitro* culture with cytokines (SCF and IL-3). The data shown are means ± standard error of the mean (SEM). (b) Upper panel: Mouse *Aml1* distal promoter regions contain potential AML1- and p53-binding motifs. The primers designed for ChIP assay of the mouse *Aml1* distal promoter region are indicated by numbers. The arrow indicates the transcription start site. Oval doublets represent two separate DNA motifs within 20 bp (black: p53-binding candidate motifs, white: AML1-binding motifs). Lower panel: ChIP assays for the detection of p53 binding and chromatin modification (methylation: H3K4me3; acetylation: H3K9Ac), as indicated in the figures. White bars: uncultured mouse bone-marrow c-Kit$^+$ cells; gray bars: c-Kit$^+$ cells after a 3-day culture. ChIP primers, corresponding to bases within the DP2 region of the *Aml1* promoter as shown in a, were used. The data shown are means ± SEM. (c) Upper panel: Primers designed for the ChIP assay of the human *AML1* distal promoter region are indicated as numbers. Lower panel: ChIP assay for detection of anti-p53 antibody binding. The data shown are means ± SEM. White bars: MOLT4 cells without IR treatment; gray bars: MOLT4 cells 2 h after IR (10 Gy) treatment. Oval doublets represent two separate DNA motifs within 20 bp (black: p53-binding candidate motifs; white: AML1-binding motifs).